On the importance of grain size in luminescence dating using quartz

Timar-Gabor, A.; Buylaert, J. P.; Guralnik, B.; Trandafir-Antohi, O.; Constantin, D.; Anechitei-Deacu, V.; Jain, M.; Murray, A. S.; Porat, N.; Hao, Q.; Wintle, A. G.

Published in:
Radiation Measurements

DOI:
10.1016/j.radmeas.2017.01.009

Publication date:
2017

Citation for published version (APA):
Timar-Gabor, A., Buylaert, J. P., Guralnik, B., Trandafir-Antohi, O., Constantin, D., Anechitei-Deacu, V., Jain, M., Murray, A. S., Porat, N., Hao, Q., & Wintle, A. G. (2017). On the importance of grain size in luminescence dating using quartz. *Radiation Measurements*, *106*, 464-471. https://doi.org/10.1016/j.radmeas.2017.01.009

Accepted Manuscript

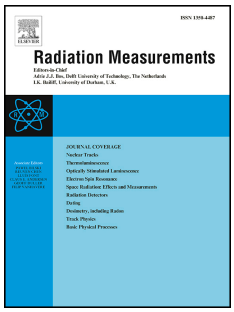

On the importance of grain size in luminescence dating using quartz

A. Timar-Gabor, J.-P. Buylaert, B. Guralnik, O. Trandafir-Antohi, D. Constantin, V. Anechitei-Deacu, M. Jain, A.S. Murray, N. Porat, Q. Hao, A.G. Wintle

PII: S1350-4487(17)30044-6

DOI: 10.1016/j.radmeas.2017.01.009

Reference: RM 5693

To appear in: *Radiation Measurements*

Received Date: 16 September 2016

Revised Date: 29 December 2016

Accepted Date: 17 January 2017

Please cite this article as: Timar-Gabor, A., Buylaert, J.-P., Guralnik, B., Trandafir-Antohi, O., Constantin, D., Anechitei-Deacu, V., Jain, M., Murray, A.S., Porat, N., Hao, Q., Wintle, A.G., On the importance of grain size in luminescence dating using quartz, *Radiation Measurements* (2017), doi: 10.1016/j.radmeas.2017.01.009.

On the importance of grain size in luminescence dating using quartz

Timar-Gabor, A.[1,2], Buylaert, J-P.[3,4], Guralnik, B.[5], Trandafir-Antohi, O.[2,6], Constantin, D.[2], Anechitei-Deacu, V.[1,2], Jain , M.[4], Murray, A.S.[3,4], Porat, N.[7], Hao, Q.[8], Wintle, A.G.[9,10]

[1]*Faculty of Environmental Sciences and Engineering, Babeş-Bolyai University, Cluj-Napoca, Romania*
[2]*Interdisciplinary Research Institute on Bio-Nano-Science, Babeş-Bolyai University, Cluj-Napoca, Romania*
[3]*Nordic Laboratory for Luminescence Dating, Department of Geoscience, Aarhus University, DTU Risø campus, Roskilde, Denmark*
[4]*Center for Nuclear Technologies, Technical University of Denmark, DTU Risø campus, Roskilde, Denmark*
[5]*Soil Geography and Landscape Group and the Netherlands Centre for Luminescence Dating, Wageningen University, Wageningen, The Netherlands*
[6]*Faculty of Physics, Babeş-Bolyai University, Cluj-Napoca, Romania*
[7]*Geological Survey of Israel, Jerusalem, Israel*
[8]*Key laboratory of Cenozoic Geology and Environment, Institute of Geology and Geophysics, Chinese Academy of Sciences, Beijing, China*
[9]*Institute of Geography and Earth Sciences, Aberystwyth University, Aberystwyth, UK*
[10]*McDonald Institute for Archaeological Research, University of Cambridge, Cambridge*

* *Corresponding author: alida.timar@ubbcluj.ro*

Abstract

There are two major problems commonly encountered when applying Optically Stimulated Luminescence (OSL) dating in the high dose range: (i) age discrepancy between different grain sizes, and (ii) age underestimation. A marked and systematic discrepancy between fine-grain (4-11 µm) and coarse-grain (63-90 µm) quartz single aliquot regeneration protocol (SAR) ages has been reported previously for Romanian and Serbian loess >40 ka (D_e of ~100 Gy), generally with fine-grain ages underestimating the depositional age. In this paper, we show a similar age pattern for two grain size fractions from Chinese loess, thus pointing to a potential worldwide phenomenon. While age underestimation is often attributed to signal saturation problems, this is not the case for fine grain material, which saturates at higher doses than coarse grains, yet begins to underestimate true ages earlier. Here we examine the dose response curves of quartz from different sedimentary contexts around the world, using a range of grain sizes (diameters of 4-11 µm, 11-30 µm, 35-50 µm, 63-90 µm, 90-125 µm, 125-180 µm, and 180-250 µm). All dose response curves can be adequately described by a sum of two saturating exponential functions, whose saturation characteristics (D_0 values) are clearly anticorrelated with grain diameter (φ) through an inverse square root relationship, $D_0=A/\sqrt{\varphi}$, where A is a scaling factor. While the mechanism behind this grain-size dependency of saturation characteristics still needs to be understood, our results show that the observation of an extended SAR laboratory dose response curve does not necessarily warrant the ability to record high doses accurately, or provide a corresponding extended age range.

Keywords

quartz; OSL; SAR; dose response; saturation characteristics; grain size

Highlights

- Discrepancy between quartz SAR-OSL ages obtained on fine and coarse grains.
- Dose response curve adequately fitted by a sum of two saturating exponentials.
- Isothermal decay fitted by a single exponential.
- Clear dependency between the saturation characteristics (D_0s) and the quartz grain size.
- No correlation between the 2 D_0 value and the maximum attainable accurate equivalent dose.

1. Introduction

A series of investigations carried out using the SAR measurement procedure (**Murray and Wintle, 2003**) on the quartz OSL signal from different grain sizes extracted from Romanian (**Timar-Gabor et al., 2011; 2012; Timar-Gabor and Wintle, 2013; Constantin et al., 2014**) and Serbian (**Timar-Gabor et al., 2015**) loess yielded intriguing results. The optical ages obtained on fine-sand sized quartz grains (63-90 µm) were reported to be systematically higher than those for silt-sized quartz grains (4-11 µm) for ages >~40 ka. It is important to note that, for all previously investigated samples with equivalent doses higher than ~100-200 Gy, the equivalent doses obtained on coarse quartz were systematically higher than for the finer material; this is unexpected when considering that the natural dose rate to fine grains should be somewhat higher than that to coarser grains (mainly because of the alpha dose rate contribution to silt-sized grains), and implies that the cause of the discrepancy resides in the equivalent dose measurements. It is also important to note that for younger ages (with equivalent doses lying in the more linear part of the dose response curves) agreement has been found between the fine and coarse grain quartz ages (**Constantin et al., 2015; Timar-Gabor et al., 2015**).

Other OSL studies carried out independently on fine and coarse grains have reported underestimations for both grain sizes for older ages (**Roberts, 2008**). For example, for Serbian loess fine quartz (4-11µm) OSL ages appear accurate back to about 50-60 ka (corresponding to a D_e of ~180 Gy), while for sediment older than this, the technique (SAR protocol) shows clear age underestimation (**Stevens et al., 2011**). Using quartz grains of 45-63 µm **Lai (2010)** reported underestimation for Luochuan loess in China for ages higher than about 70 ka. Using 63-90 µm

quartz, **Buylaert et al**. (**2008**) suggested that one should be careful when dating Chinese loess samples with SAR on sand-sized quartz for which the D_e values exceed 120 Gy (~40 ka).

Different saturation characteristics for the fine and coarse quartz fractions extracted from loess have also been reported before, with the fine grains showing higher saturation characteristics (see **Constantin et al.** (**2012**)**; Timar-Gabor et al.** (**2012**)**; Timar-Gabor et al.** (**2015**)). This behaviour was found to be characteristic of other sedimentary contexts as well, such as the Paleolithic sequence at an archaeological site in Northeastern Romania (**Trandafir et al., 2015**). This is particularly intriguing when juxtaposed with the fact that underestimation of age commences earlier in the fine fraction, than in the coarse. Also, it is noteworthy that the saturation characteristics that we have obtained before for both the fine and the coarse quartz fraction are very similar to the values reported elsewhere in the literature, regardless of location (see **Timar-Gabor et al.** (**2012**)). The existence of a 'standardized' dose response curve has been shown for both post-IR OSL from polymineral fine grains and OSL from chemically-purified coarse-grained quartz (**Roberts and Duller, 2004**). Another standardized dose response curve has been previously obtained for 38-63 μm quartz chemically extracted from samples of loess from China, North America, North Africa and Europe by **Lai et al. (2007**), while for the same grain size **Long et al. (2010)** obtained a standardized dose response curve for sediments of lacustrine origin. However, these studies did not consider the dose response region where the signals approach saturation.

Assuming an exponentially saturating growth of the signal where the luminescence intensity at dose D is a function of the maximum luminescence intensity, the radiation dose, and a characteristic dose D_0 (a parameter that describes how rapidly the signal reaches saturation), **Wintle and Murray (2006)** recommended $2\times D_0$ (~86% of full saturation) as an upper limit for determining meaningful equivalent doses. However, their recommendation was based only on concerns regarding precision; for higher natural doses any uncertainty in the natural luminescence signal would result in a large and asymmetric uncertainty in the interpolated equivalent dose.

While the maximum measurable equivalent dose is of course limited by saturation of the laboratory dose response, in general the reported underestimation in the previously mentioned studies was not associated with a proximity of natural signals to the laboratory saturation level for any of the grain sizes used. Also, as reported by **Wintle and Murray (2006)** when higher

doses (e.g. above 125 Gy) are employed to construct the dose–response curve an additional linear, component can occur. This component has since been shown to be the early expression of at least a second saturating exponential function (**Murray et al., 2007; Lowick et al., 2010; Timar-Gabor et al., 2012**)

To summarise, the dose at which age underestimation becomes significant cannot be easily generalised based on existing data; this limit depends not only on the laboratory saturation characteristics and the dose rate, but also on the grain size used for dating.

In this work we investigate the saturation characteristics of the SAR dose response curve constructed using fast-component quartz OSL from various grain sizes from different sedimentary contexts and locations around the world, in order to assess whether there is a potential dependence between saturation characteristics and the grain size, with the ultimate aim of gaining more knowledge on the maximum dose which can be accurately determined using the OSL signal from quartz.

2. Samples, instrumentation and measurement protocol

Experiments presented in the current study have been conducted on archived quartz separates of different grain sizes from our previous investigations as well as newly processed samples. Samples of quartz extracted from loess are as follows. Samples coded as MV were collected from the Mircea Vodă loess-paleosol section in Dobrudjea, Romania (**Timar et al., 2010; Timar-Gabor et al., 2011)**. CAC is the code for samples from the section at Caciulatesti in southern Romania (**Constantin et al., 2012**). MST is the laboratory code used at the Mostistea section from the Romanian Plain (**Vasiliniuc et al., 2011; Timar-Gabor et al., 2012**). CST samples were taken from Costineşti section near the Black Sea shore (**Timar-Gabor and Wintle, 2013; Constantin et al., 2014**), samples coded as LCA come from Lunca section in South Western Romania (**Constantin et al., 2015**), samples coded as ORL are quartz extracts from Serbian loess (**Timar-Gabor et al., 2015**), while samples coded with XF come from Xifeng section in the Chinese loess plateau **(Hao et al., 2012, 2015)** (see details in the supplementary material). In addition samples with an origin other than loess have been investigated. Sample coded as RUH comes from Ruhama desert loess section in Israel (**Wieder et al., 2008**), sample coded as M#6 is quartz extracted from a carbonate eolianite from Eivissa (see **del Valle et al., 2016** for the geological context), sample S1 is eolian sand from the Danube

Delta (**Preoteasa et al., 2016**). Also, samples of marine sediments from the Eemian site at Sula in Russia (**Murray et al., 2007**), a sample of sand at Gammelmarke in southern Jutland (**Murray and Funder, 2003**) and sand from Skagen (**Murray et al., 2015**), both in Denmark, and a sample of sand from Zwolle, Netherlands (**Buylaert et al., 2009, 2012**) have been included in the analysis. Samples of grain size larger than 35 µm have been obtained by sieving while for grains smaller than 30 µm settling using Stokes' law was used. Hydrofluoric acid was used for etching grains larger than 63 µm while for the smaller grain sizes hydrofluorosilicic acid was employed.

Continuous wave optically stimulated luminescence (CW-OSL) measurements on quartz were made on Risø TL/OSL DA-20 readers (**Thomsen et al., 2006)** in Cluj-Napoca, Romania, and at DTU Nutech/Nordic Laboratory for Luminescence Dating (Aarhus University) located on DTU Risø campus (Denmark). Blue light emitting diodes (LEDs) emitting at 470±30 nm were used for stimulation and luminescence signals were observed through a 7.5 mm thick Hoya U-340 UV filter. Grain sizes of 4-11 µm and 11-30 µm were deposited on aluminium disks while the 35-50 µm and coarser fractions were mounted on stainless steel disks. Irradiations were carried out using a ^{90}Sr-^{90}Y beta source. The dose rate was calibrated for fine grains deposited on aluminium disks and coarse grains on stainless steel disks using fine (4-11 µm) and coarse (180-250 µm) quartz supplied (**Hansen et al., 2015**). The OSL signal was collected in time intervals of 0.154 s. All samples have been analysed using the SAR procedure (**Murray and Wintle, 2000, 2003**). The OSL signal used for analysis was that obtained for the first 0.308 s of the decay curve minus a background derived from the signal measured between 2.464 and 3.080 s; these integration intervals were used in our previous studies. In our protocol, natural and regenerated signals were measured after a preheat of 10 s at 220°C; the corresponding OSL responses to a test dose (17 Gy) were measured after a cutheat (ramp heating) to 180°C. The value of the test dose (17 Gy) was kept constant through all measurements for all grain sizes of quartz in order to facilitate the direct comparison of the dose response curves. A high-temperature bleach was performed by stimulating with the blue diodes for 40 s at 280°C (**Murray and Wintle, 2003**).

3. Results and discussion

3.1. The age discrepancy

In order to illustrate the problems of age discrepancy and age underestimation **figure 1** shows a comparison between the ages previously obtained using fine (4-11 µm) and coarse (63-90 µm) quartz from three representative loess paleosol sequences in Romania and Serbia (Costinesti- **Constantin et al., 2014; Timar-Gabor and Wintle, 2013;** Lunca- **Constantin et al., 2015;** Orlovat-**Timar-Gabor et al., 2015**) and from the representative Xifeng section in China. Details on Xifeng section and the chronology presented are given in the supplementary material.

The OSL chronologies using our SAR protocol applied to different grain-sizes of quartz are consistent up to equivalent doses of approximately 100 Gy (equivalent to OSL ages of <40 ka). For loess samples with equivalent doses beyond approximately 100 Gy, the OSL ages on fine quartz underestimate those yielded by coarse quartz and the degree of underestimation increases with age.

3.1.1. Thermal stability of the signal

One of the possible causes for age underestimation in luminescence dating is the thermal loss of the signal during its build-up (**Christodoulides et al., 1971**). Although thermal instability is typically addressed through routine preheat plateau tests, the thermal lifetime of the target OSL dosimetric trap used for dating is seldom explicitly determined.

Isothermal luminescence decay experiments were carried out in order to quantify the thermal stability of the dosimetric trap for samples of different grain sizes from Costineşti. After an initial bleaching, each aliquot was irradiated with 170 Gy and isothermally stored at elevated temperatures (200, 220, 240°C) for various holding times (up to 10^5 s at 200°C), followed by OSL signal readout using the SAR-OSL protocol. The OSL response to a test dose of 17 Gy was used for sensitivity correction.

The time-evolution of the normalized OSL signal L(t) (a.u.) at a temperature T (K) is illustrated in **figure 2** and was found to be best described by a single decaying exponential function of the form:

$$L(t) = L_{max}\exp(-\mathrm{s}\exp(-\mathrm{E}/(\mathrm{k_B}\,\mathrm{T}))\,\mathrm{t}) \quad (1)$$

Where L_{max} is the initial sensitivity-corrected OSL light sum, E (eV) and s (s^{-1}) are the Arrhenius parameters (activation energy and frequency factor, respectively), k_B (eV K^{-1}) is Boltzmann's constant and t (s) is the holding time at temperature T. Trap lifetime was derived using the equation:

$$\tau = s^{-1} \exp(E/(k_B T)) \quad (2)$$

Different kinetic parameters were obtained for the fine and coarse grain quartz, but our results fall in the range of previous studies (see **Table 1** for a summary).

Trap lifetimes for both investigated samples are well beyond the age of interest for dating purposes: ~230 Ma for fine quartz and ~15 Ga for coarse quartz. Consequently, our data are not consistent with the hypothesis that the observed age discrepancy between the two grain sizes is a result of thermal instability of the signal.

3.1.2. Dose response curves

Considering a sample with N electron traps, irradiated with a dose rate r = D/t, ignoring thermal drainage (as justified in the previous section), the total number of traps filled at time t is:

$$n = N\,(1 - \exp(-rpt)) \quad (3)$$

Where p is the probability per unit dose for a population of traps being filled (**Durrani et al., 1977**). Thus, for a certain dose:

$$n\,(D) = N\,(1 - \exp(-pD)) \quad (4)$$

Assuming that the probability of a trapped electron recombining to give a luminescence photon is independent of dose, this dependence results in single exponential growth of the signal often reported in OSL dating studies:

$$L(D) = L_{max}(1 - \exp(-D/D_0)) \quad (5)$$

As such, D_0 values can be interpreted as the inverse value of the probability of a population of traps being filled per unit dose. The higher the D_0 values, the higher the dose at which saturation occurs and the smaller the fraction of traps filled per unit dose.

Our previous studies have shown however that, in the high dose range the dose response curves of quartz cannot be fitted satisfactorily by a single saturating exponential and a sum of two such functions has to be used (**Timar-Gabor et al., 2012**).

$$L(D) = L_{1max}(1 - \exp(-D/D_{01})) + L_{2max}(1 - \exp(-D/D_{02})) \quad (6)$$

While the physical meaning of the two components is yet unknown, the D_{01} and D_{02} values obtained for fine grains are markedly different from D_{01} and D_{02} of coarse grain material (**Timar-Gabor et al., 2012; Hansen et al., 2015)**.

Figure 3 presents a comparison of SAR dose response curves for fine and coarse quartz from two sections in Romania and for loess from Xifeng. It appears that these Chinese loess coarse

grains also reach saturation at lower doses than the corresponding fine grains. However, coarse grains from Romanian and Chinese loess follow the same trend, as do the fine grains. For the coarse grains, the regenerated signal reaches 86% of saturation level (equivalent to the 2 D_0 limit for a single saturating exponential growth) for doses of ~350 Gy, whereas for the 4-11 μm quartz the regenerated signals do not reach ~86% of saturation until ~2000 Gy.

For these particular aliquots the ratio between the amplitude of the two components (L_{1max}/L_{2max}) ranges between 0.5 and 1 for both grain sizes; the D_0 values for the two exponentials for the 4-11μm grains and for the 63-90μm are given in **Table 2** for samples from 3 sections, CST, MV and XF. It is also important to note that the two fitted D_0 values for each curve differ by an order of magnitude and so it is unlikely that these components are fitting artifacts **(Istratov and Vyvenko, 1999)**. It is also interesting to note that the dose response curves of the two grain sizes overlap up to doses of about 100 Gy. As mentioned, ages obtained for the two grain sizes are in good agreement up to about this level of equivalent dose. There is a degree of scatter among the values obtained for a given grain size, which is to be expected due to the different origins of quartz. However, the values for a particular grain size are markedly different from those of the other grain size no matter what sample is investigated; this can be seen from **figure S4**, which compares different aliquots of quartz of 4-11μm and 63-90 μm grains.

3.2. Dose response curves of various grain sizes of quartz from different geological contexts.

We have also investigated the dose response curves of different grain sizes of quartz of different origins. For all the coarse (≥35 μm) grain measurements, the grains were mounted on stainless steel disks and the same dose rate has been used (no significant change in dose rates for grains ≥40 μm expected; **Armitage and Bailey, 2005)**. For the 11-30 μm grains deposited on aluminum disks the same dose rate as determined for 4-11 μm grains was used. Based on the observations of **Armitage and Bailey (2005)** this might be a slight underestimation, but the bias is less than ~4% and unlikely to be of significance in these experiments. The results are summarised in **figure 4**, and a clear trend of increasing saturation dose with decreasing grain size can be seen.

In order to quantify this dependence, the average D_0 values for multiple aliquots of different grain sizes were first calculated. Dose response curves were constructed using a minimum of 10

points up to at least 2500 Gy (grains >63 μm); for finer material dose response curves were constructed up to at least 5000 Gy. These very high doses were necessary since the choice of the maximum dose point used to construct the dose response curve influences the values of the parameters obtained if the dose response curve is not constructed up to full saturation (**figure 5**). It can be seen that the values obtained for the fitting parameters depend on the maximum dose until the dose response curve reaches full saturation, when the D_0 values also reach a plateau.

A total of 99 aliquots of different grain sizes were used, the relevant information being presented in **table 3**. Each aliquot considered in the analysis successfully passed recycling (**Murray and Wintle, 2003**) and IR depletion ratio tests (**Duller, 2003**).

The average obtained D_0 values (Gy) are plotted against the average grain diameter φ (μm) in **figure 6**. The linear trend observed in **figure 6** on a log-log scale translates to a power-law dependency, in which the exponent of the power function is determined by the slope and the scaling factor by the intercept. Independent and unconstrained fits of the D_{01} and D_{02} datasets using $D_{0x} = A\varphi^B$, yielded identical (within error) best-fit exponents of $B = -0.49 \pm 0.07$ for D_{01} and $B = -0.52 \pm 0.06$ for D_{02}. Since in both cases, the regressed exponents consistent with a square root (B = -0.5), we find it plausible to simplify the initially anticipated power-law to an inverse square root relationship, namely $D_{0x} = A/\sqrt{\varphi}$. Consequently, each of the datasets was refitted with a fixed B = -0.5, to obtain only the scaling factor A (with units of (Gy $m^{-0.5}$). These fits (**figure 6)** yielded best-fit values of $A_{01} = 0.46 \pm 0.03$Gy $m^{-0.5}$ and $A_{02} = 4.4 \pm 0.3$Gy $m^{-0.5}$, which are separated by a factor of ~10 (corresponding to a typical D_{02} / D_{01} ratio).

Reports of a dependence of saturation characteristics upon grain size have, to the best of our knowledge, not been documented in the literature, and an underlying physical mechanism (i.e. the increase of characteristic dose, and the decrease in trap filling probability, with decreasing grain size) remains yet unknown.

Investigations of TL emission as function of particle size have been performed on LiF (**Burlin et al., 1969**) and Al_2O_3:C (**Akselrod et al., 1993**). In their studies, a decrease in the luminescence intensity is reported with decreasing grain size. On the other hand, in the case of nanoparticles, generally an increase in the TL output is reported as the particle size is decreased (see as an example **Chen et al., 1997** for ZnS nanoparticles). As the particles become smaller the surface/volume ratio increases and so does the importance of surface defects. By comparing the OSL output (absolute number of counts) for a certain dose for fine (4-11μm) and coarse (63-90

µm) grains, the fine grains of sedimentary quartz have, in general, higher light output per unit mass than coarse grains. However, examination of the existence of a trend between the light levels obtained for a certain dose per unit mass and grain size not possible from the available dataset. Further investigations will aim at obtaining a better understanding of the role of surface defects in OSL production and any related dose dependence.

4. Conclusions

The good agreement of the ages obtained using different grain sizes of quartz in the low dose range increases our confidence in the accuracy of the SAR-OSL ages for samples with equivalent doses of about 100 Gy or less, as further confirmed by comparison with independent age control provided through tephrochronology (**Constantin et al., 2012; Anechitei-Deacu et al., 2014**) or radiocarbon dating (**Trandafir et al., 2015**). On the other hand, the age discrepancy of SAR-OSL ages previously reported for Romanian and Serbian loess for ages beyond ~40 ka (equivalent doses >~100 Gy) was also found to be characteristic of Chinese loess. It is thus believed that this is potentially a global phenomenon, affecting previously-obtained chronologies worldwide, and further increasing concerns for the accuracy of silt-sized SAR-OSL ages in this high dose range.

We have shown that underestimation of the fine grains ages cannot be attributed to thermal instability of the signal, but is more likely related to a hitherto unknown dose dependent phenomenon.

The overlap observed between the SAR laboratory dose response curves of quartz of different grains from different geological contexts as well as of different grain sizes up to 100 Gy confirm the validity of the standardized dose response curve concept (**Roberts and Duller, 2004; Li et al., 2015**) for the linear region of the dose response curve.

However, with regard to the dose level at which saturation is reached, we find that the saturation characteristics (D_0 values) are related to grain diameter via an inverse square root relationship of the form $D_0 = A/\sqrt{\varphi}$, where in the characteristic dose increases for smaller grain sizes. Based on this observation, together with the underestimation generally reported for smaller grain sizes, we suggest that, at least for quartz samples that display a dose response curve that is described by a sum of two saturating exponential functions, it is not possible at present to provide a limit for dating in terms of values of the D_0 of either component.

Acknowledgement:
A. Timar-Gabor, D. Constantin, V. Anechitei-Deacu have received funding from the European Research Council (ERC) under the European Union's Horizon 2020 research and innovation programme ERC-2015-STG (grant agreement No [678106]). J-P. Buylaert has received funding from the European Research Council (ERC) under the European Union's Horizon 2020 research and innovation programme ERC-2014-STG (grant agreement No [639904]).

B. Guralnik was supported by the Netherlands Organisation for Scientific Research (NWO) VENI grant 863.15.026.
The authors would like to thank Reuven Chen and David Huntley for discussions on the dependence of luminescence characteristics on grain sizes, and an anonymous reviewer for a careful reading of the manuscript.

REFERENCES

1. Akselrod, M.S., Kortov V.S., Gorelova, E.A., 1993. Preparation and properties of Al_2O_3:C. Radiation Protection Dosimetry 47, 159-164.
2. Anechitei-Deacu, V., Timar-Gabor, A., Fitzsimmons, K.E., Veres, D., Hambach, U., 2014. Multi-method luminescence investigations on quartz grains of different sizes extracted from a loess section in southeast Romania interbedding the Campanian Ignimbrite ash layer. Geochronometria 41, 1-14.
3. Armitage, S.J., Bailey, R.M., 2005. The measured dependence of laboratory beta dose rates on sample grain size. Radiation Measurements 39, 13-127.
4. Burlin, T.E., Chan, F.K., Zanelli, G.D., Spiers, F.W., 1969. Effect of particle size on the thermoluminescence of lithium fluoride. Nature 221, 1047-1048.
5. Buylaert, J.P., Murray, A.S., Vandenberghe, D., Vriend, M., De Corte, F., Van den haute, P., 2008. Optical dating of Chinese loess using sand-sized quartz: Establishing a time frame for Late Pleistocene climate changes in the western part of the Chinese Loess Plateau. Quaternary Geochronology 3, 99-113.
6. Buylaert, J.P., Murray, A.S., Thomsen, K.J., Jain, M., 2009. Testing the potential of an elevated temperature IRSL signal from K-feldspar. Radiation Measurements 44, 560-565.
7. Buylaert, J. P., Jain, M., Murray, A.S., Thomsen, K.J., Thiel, C., Sohbati, R., 2012. A robust feldspar luminescence dating method for Middle and Late Pleistocene sediments. Boreas 41, 435-451.
8. Chen, W., Wang, Z., Lin, Z., Lin, L., 1997. Thermoluminescence of ZnS nanoparticles. Applied Physics Letters 70 (11), 1465-1467.

9. Christodoulides, C., Ettinger, K.V., Fremlin, J.H., 1971. The use of TL glow peaks at equilibrium in the examination of the thermal and radiation history of materials. Modern Geology 2, 275-280.
10. Constantin, D., Timar-Gabor, A., Veres, D., Begy, R., Cosma, C., 2012. SAR-OSL dating of different grain-sized quartz from a sedimentary section in southern Romania interbedding the Campanian Ignimbrite/Y5 ash layer. Quaternary Geochronology 10, 81-86.
11. Constantin, D., Begy, R., Vasiliniuc, S., Panaiotu, C., Necula, C., Codrea, V., Timar-Gabor, A., 2014. High-resolution OSL dating of the Costineşti section (Dobrogea, SE Romania) using fine and coarse quartz. Quaternary International 334-335, 20-29.
12. Constantin, D., Cameniţă, A., Panaiotu, C., Necula, C., Codrea, V., Timar-Gabor, A., 2015. Fine and coarse-quartz SAR-OSL dating of Last Glacial loess in Southern Romania. Quaternary International 357, 33-43.
13. Duller, G.A.T., 2003. Distinguishing quartz and feldspar in single grain luminescence measurements. Radiation Measurements 37, 161-165.
14. Durrani, S.A., Groom, P.J., Khazal, K.A.R., McKeever, S.W.S., 1977. The dependence of the thermoluminescence sensitivity upon the temperature of irradiation in quartz. Journal of Physics D: Applied Physics 10, 1351-1361.
15. Hansen, V., Murray, A., Buylaert, J.-P., Yeo, E.-Y., Thomsen, K., 2015. A new irradiated quartz for beta source calibration. Radiation Measurements 81, 123-127.
16. Hao, Q.Z., Wang, L., Oldfield, F., Peng, S.Z., Qin, L., Song, Y., Xu, B., Qiao, Y.S., Bloemendal, J., Guo, Z.Z., 2012. Delayed build-up of Arctic ice sheets during 400,000-year minima in insolation variability. Nature 490, 393-396.
17. Hao, Q.Z., Wang, L., Oldfield, F., Guo, Z.T, 2015. Extra-long interglacial in Northern Hemisphere during MISs 15-13 arising from limited extent of Arctic ice sheets in glacial MIS 14. Scientific Reports 5: 12103, doi:10.1038/srep12103.
18. Huntley, D.J., Short, M.A., Dunphy, K., 1996. Deep traps in quartz and their use for optical dating. Canadian Journal of Physics 74, 81-91.
19. Istratov, A., Vyvenko, O.F., 1999. Exponential analysis in physical phenomena. Review of Scientific Instruments 70, 1233-1257.
20. Lai, Z.P.,2010. Chronology and the upper dating limit for loess samples from Luochuan section in the Chinese Loess Plateau using quartz OSL SAR protocol. Journal of Asian Earth Sciences 37, 176-185.
21. Lai, Z.-P., Fan, A.C., 2013. Examining quartz OSL age underestimation for loess samples from Luochuan in the Chinese Loess Plateau. Geochronometria 41, 57-64.
22. Lai, Z.P., Brückner, H., Zöller, L., Fülling, A., 2007. Existence of a common growth curve for silt-sized quartz OSL of loess from different continents. Radiation Measurements 42, 1432-1440.

23. Li, S-H., Chen, G., 2001. Studies of thermal stabilities of trapped charges associated with OSL from quartz. Journal of Physics D: Applied Physics 34, 493-498.
24. Li , B., Roberts, R.G., Jacobs, Z., Li, S.-H., 2015. Potential of establishing a global standardised growth curve (gSGC) for optical dating of quartz from sediments. Quaternary Geochronology 27, 94-104.
25. Long, H., Lai, Z.P., Fan, Q.S., Sun, Y.J., Liu, X.J., 2010. Applicability of a quartz OSL standardised growth curve for D_e determination up to 400 Gy for lacustrine sediments from the Qaidam Basin of the Qinghai-Tibetan Plateau. Quaternary Geochronology 5, 212-217.
26. Lowick, S.E., Preusser, F., Wintle, A.G., 2010. Investigating quartz optically stimulatedluminescence dose-response curves at high doses. Radiation Measurements 45,975-984.
27. Murray, A.S., Wintle, A.G., 1999. Isothermal decay of optically stimulated luminescence in quartz. Radiation Measurements 30,119-125.
28. Murray, A.S., Wintle, A.G., 2000. Luminescence dating of quartz using an improved single-aliquot regenerative-dose protocol. Radiation Measurements 32, 57-73.
29. Murray, A.S., Wintle, A.G., 2003. The single aliquot regenerative dose protocol: potential for improvements in reliability. Radiation Measurements 37, 377-381.
30. Murray, A.S., Funder, S., 2003. Optically stimulated luminescence dating of the Danish Eemian coastal marine deposit: a test of accuracy. Quaternary Science Reviews 22, 1177-1183.
31. Murray, A.S., Svendsen, J.I., Mangerud, J., Astakhov, V.I., 2007. Testing the accuracy of quartz OSL dating using a known-age Eemian site on the river Sula, northern Russia. Quaternary Geochronology 2, 102-109.
32. Murray, A., Buylaert, J.P., Thiel, C., 2015. A luminescence dating comparison based on a Danish beach-ridge sand. Radiation Measurements 81, 32-38.
33. Preoteasa, L., Vespremeanu-Stroe, A., Tătui, F., Zăinescu, F., Timar-Gabor, A., Cârdan, I., 2016. The evolution of an asymmetric deltaic lobe (sf. Gheorghe, Danube) in association with cyclic development of the river-mouth bar: Long-term pattern and present adaptations to human-induced sediment depletion. Geomporphology 253, 59-73.
34. Roberts, H.M., Duller, G.A. T., 2004.Standardised growth curves for optical dating of sediments using multiple-grain aliquots. Radiation Measurements 38, 241-252.
35. Roberts, H.M., 2008. The development and application of luminescence dating to loess deposits: a perspective on the past, present and future. Boreas 37, 483-507.
36. Singarayer, J.S., Bailey, R.M., 2003. Further investigations of the quartz optically stimulated luminescence components using linear modulation. Radiation Measurements 37, 451-458.

37. Smith, B. W., Rhodes, E. J., Stokes, S., Spooner, N. A., 1990. The optical dating of sediments using quartz. Radiation Protection Dosimetry34, 75-78.
38. Stevens, T., Marković, S.B., Zech, M., Hambach, U., Sümegi, P., 2011. Dust deposition and climate in the Carpathian Basin over an independently dated last glacial–interglacial cycle. Quaternary Science Reviews 30, 662-681.
39. Thomsen, K.J., Bøtter-Jensen, L., Denby, P.M., Moska P., Murray, A.S., 2006. Developments in luminescence measurement techniques. Radiation Measurements 41, 768-773.
40. Timar, A.,Vandenberghe, D., Panaiotu, E.C., Panaiotu, C.G., Necula, C., Cosma, C.,Van den haute, P., 2010. Optical dating of Romanian loess using fine-grained quartz. Quaternary Geochronology *5*, 143-148.
41. Timar-Gabor, A., Vandenberghe, D.A.G., Vasiliniuc, S., Panaoitu, C.E., Panaiotu, C.G., Dimofte, D., Cosma, C., 2011. Optical dating of Romanian loess: A comparison between silt-sized and sand-sized quartz. Quaternary International 240, 62-70.
42. Timar-Gabor, A., Vasiliniuc, Ş., Vandenberghe, D.A.G., Cosma, C., Wintle, A.G., 2012. Investigations into the reliability of SAR-OSL equivalent doses obtained for quartz samples displaying dose response curves with more than one component. Radiation Measurements 47, 740-745.
43. Timar-Gabor, A., Wintle, A.G., 2013. On natural and laboratory generated dose response curves for quartz of different grain sizes from Romanian loess. Quaternary Geochronology 18, 34-40.
44. Timar-Gabor, A., Constantin, D., Marković, S.B., Jain, M., 2015. Extending the area of investigation of fine versus coarse quartz optical ages from the Lower Danube to the Carpathian Basin. Quaternary International 388, 168–176.
45. Trandafir, O., Timar-Gabor, A., Schmidt, C., Veres, D., Anghelinu, M., Hambach, U., Simon, S., 2015. OSL dating of fine and coarse quartz from a Palaeolithic sequence on the Bistrița Valley (Northeastern Romania). Quaternary Geochronology 30, 487-492.
46. del Valle, L., Gomez-Pujol, L., Fornos, J.J., Timar-Gabor, A., Anechitei-Deacu, V., Pomar, F., 2016.Middle to Late Pleistocene dunefields in rocky coast settings at Cala Xuclar (Eivissa, WesternMediterranean): recognition, architecture and luminescence chronology. Quaternary International 407, 4-13.
47. Vasiliniuc, S., Timar-Gabor, A., Vandenberghe, D.A.G., Panaiotu, C.G., Begy, R. Cs., Cosma, C., 2011. A high resolution optical dating study of the Mostiştea loess-palaeosol sequence (SE Romania) using sand-sized quartz. Geochronometria 38, 34-41.
48. Wieder, M., Gvirtzman, G., Porat, N., Dassa, M., 2008. Paleosols of the southern coastal plain of Israel. Journal of Plant Nutrition and Soil Science 171, 533-541.

49. Wintle, A.G., Murray, A.S., 1998. Towards the development of a preheat procedure for OSL dating of quartz. Radiation Measurements 29, 81-94.
50. Wintle, A.G., Murray, A.S., 2006. A review of quartz optically stimulated luminescence characteristics and their relevance in single-aliquot regeneration dating protocols. Radiation Measurements 41, 369-391.

Table captions

Table 1. Trap parameters for loess samples in this study, as well as others reported in the literature for comparison.

Table 2. Dose saturation characteristics when using a sum of two exponential functions

Table 3. Information on samples used to derive the average saturation characteristics.

Figure captions

Figure 1. Plot of SAR OSL ages obtained on fine (4-11 µm; squares) quartz and coarse (63-90 µm; circles) quartz for representative loess-paleosol sequences. Ages increase with depth for both grain sizes. The Holocene soil (S0) and Last Interglacial soil S1 are shaded. Based on the correlation of S1 with MIS 5, samples which are stratigraphically below S1 should be older than 130 ka.

Figure 2. Isothermal decay of the fine (4-11 µm; sample CST 2) and coarse (63-90 µm; sample CST 22) quartz OSL signal with best-fitting curves (95% confidence intervals shaded) and fitting residuals shown below. Combining the data for fine and coarse data (right panel) is also inadequate, as seen by segregation of the residuals by dataset; hence the different best-fit parameters for each grain size fraction are considered as genuine.

Figure 3. Representative SAR dose response curves for fine (4-11 µm) and coarse (63-90 µm) quartz from Romanian loess and Chinese loess.

Figure 4. Representative SAR dose response curves of quartz of different grain sizes and origins.

Figure 5. Comparison of D_0 values for D_{01} (a) and D_{02} (b) obtained for fine (M#6) and coarse grains (MV8) of quartz as function of the maximum given dose.

Figure 6. Variation of saturation characteristics (D_0 parameters) as function of grains size. Please note the log-log scale.

TABLE 1. Trap parameters for loess samples in this study, as well as others reported in the literature for comparison.

Reference	Sample type	Natural/ Lab irradiated	Grain size (μm)	Fitting function	E (eV)	$\log_{10}$S (S in s^{-1})	Lifetime at 20°C (Ma)
Smith et al., 1990.	Sediment Oxfordshire	Lab irradiated	either 90 – 125or 125 – 180	Sum of 2 exp (second component is negligible)	1.84±0.07	15.3±0.7	~ 600
Huntley et al., 1996.	Sand from beach dunes, Australia	Natural	~ 100	Sum of 4 exp (contributions of 20, 20, 49 and 1%)	1.39±0.27 1.55±0.07 1.65±0.01 1.82±0.05	12±3 12.9±0.7 13.4±0.1 14.1±0.5	0.014 2 28 4700
Wintle and Murray, 1998.	Aeolian sand, Australia	Natural	90 – 125	Sum of 2 exp (contribution of >99 and <1%)	1.88±0.03 2.00±0.3	15.9±0.3 16±3	~ 850 ~76650
Murray and Wintle, 1999.	Aeolian sand, Australia	Lab irradiated	90 – 125	Sum of 3 exp (contribution of 64, 34 and 2%)	1.66±0.03 1.14±0.14 1.75±0.15	13.0±0.3 9.5±1.5 13.4±1.5	~110 0.0004 1500
Li and Chen, 2001.	Alluvial sediment Hong Kong	Natural Lab irradiated	125 – 180	Sum of 2 exp	OSL trap: 1.87 R trap: 1.32 OSL trap: 1.96 R trap: 1.39	15.0 11.0 15.8 11.9	3.25 0.014 24.4 0.03
Singarayer and Bailey, 2003.	Various sedim. samples	Lab irradiated	either 90 – 125 or 125 – 180	Sum of 5 exp * LM-OSL	Fast: 1.74 Medium: 1.8 S1: 2.02 S2: 1.23	13.9 13.2 14.8 10.7	310 19000 2610000 0.001
Lai and Fan, 2013.	Loess, China	Lab irradiated	45 – 63	Sum of 2 exp (parameters for the second component not mentioned)	1.48	12.7	0.31
This study	Loess, Romania	Lab irradiated	4 – 11 63 – 90	1 exp 1 exp	1.68±0.03 1.97±0.03	13.0±0.3 16.2±0.3	~230 ~14750

TABLE 2. Dose saturation characteristics when using as sum of two exponential functions

Grain diameter (μm)	Sample code	D_{01} (Gy)	D_{02} (Gy)
4-11	CST	141±15	1386±109
	MV	131±20	1250±121
	XF	214±30	1888±405
63-90	CST	33±44	246±83
	MV	53±6	550±42
	XF	45±9	244±21

TABLE3. Information on samples used to derive the average saturation characteristics.

Grain diameter (μm)	Number of aliquots used	Sample type	D_{01} (Gy)	D_{02} (Gy)
4-11	36	14 aliquots Romanian loess (MV, CAC, CST, MST, LCA) 2 aliquots Serbian loess (ORL) 2 aliquots Ruhama Israeli desert loess (RUH) 7 aliquots eolianite from Eivissa (M#6) 11 aliquots loess Xifeng, China (XF)	151±5	1411±64
11-30	5	Romanian loess (CST)	129±8	1197±94
35-50	6	Romanian loess (MV)	82±6	901±113
63-90	24	15 aliquots Romanian loess (MV, CAC, CST, MST, LCA) 2 aliquots eolianite from Eivissa (M#6) 7 aliquots loess Xifeng, China (XF)	44±2	452±32
90-125	12	1 aliquot Romanian loess (CAC) 2 aliquots eolianite from Eivissa (M#6) 4 aliquots Ruhama Israeli desert loess (RUH) 2 aliquots sand from the Danube delta 3 aliquots sand from Gammelmarke in southern Jutland	36±3	363±55
125-180	8	1 aliquot Romanian loess (CAC) 1 aliquot sand from Skagen 3 aliquots eolianite from Eivissa (M#6) 3 aliquots sand from the Danube delta	37±3	361±45
180-250	8	2 aliquots eolianite from Eivissa (M#6) 3 aliquots sand from Zwolle, Netherlands 3 aliquots marine sediments from the Eemian site from Sula	41±4	305±105

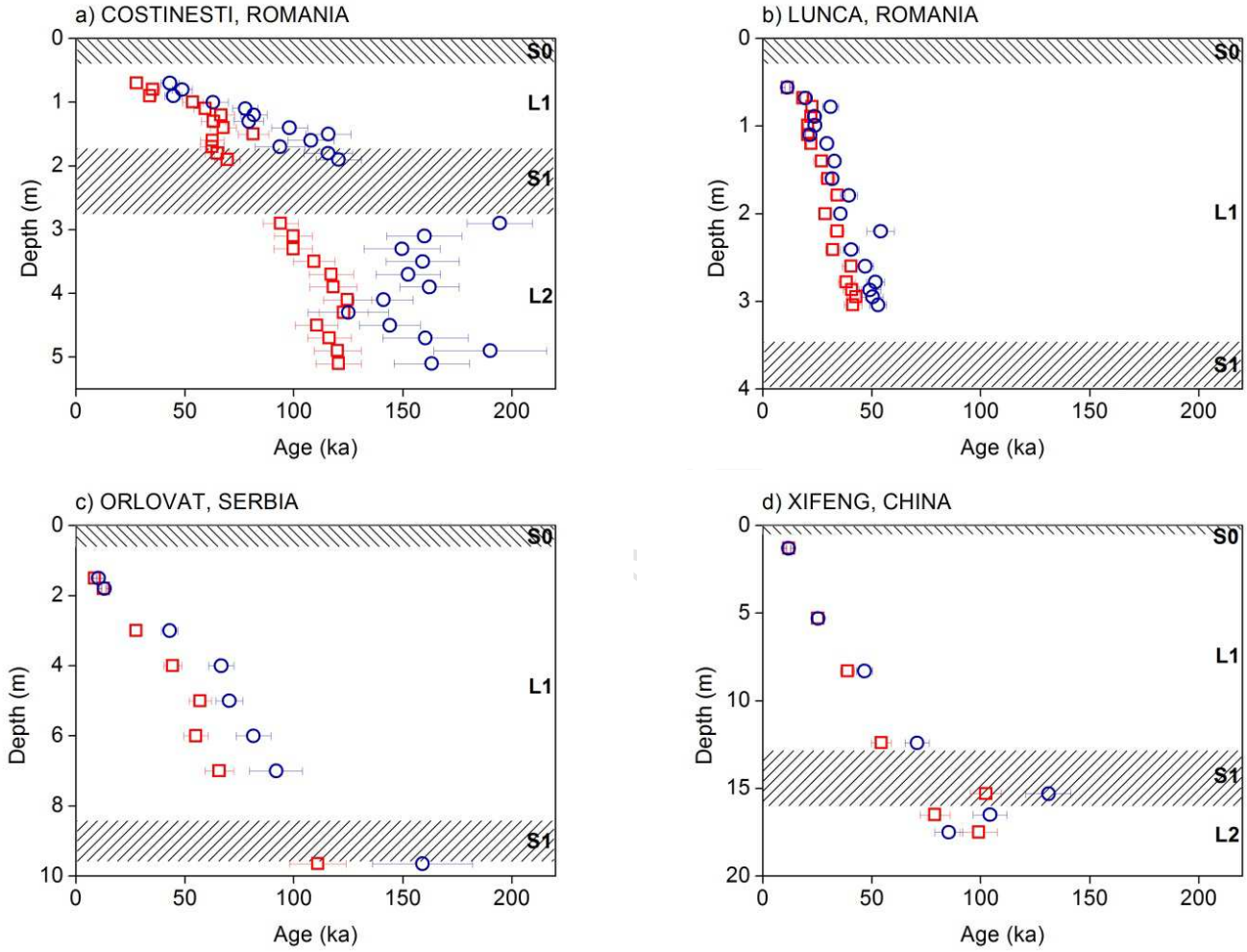

FIGURE 1. Plot of SAR OSL ages obtained on fine (4-11 µm; squares) and coarse (63-90 µm; circles) quartz for representative loess-paleosol sequences. Ages increase with depth for both grain sizes. The Holocene soil (S0) and Last Interglacial soil S1 are shaded. Based on the correlation of S1 with MIS 5, samples which are stratigraphically below S1 should be older than 130 ka.

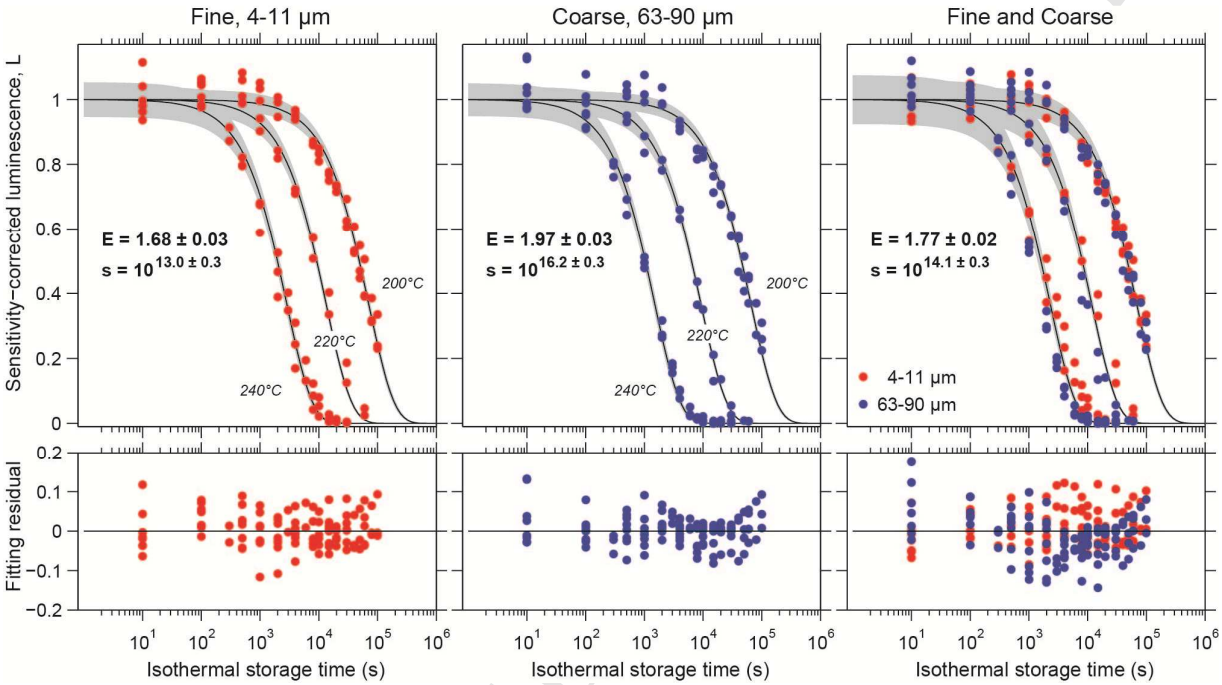

FIGURE 2. Isothermal decay of the fine (4-11 µm; sample CST 2) and coarse (63-90 µm; sample CST 22) quartz OSL signal with best-fitting curves (95% confidence intervals shaded) and fitting residuals shown below. Combining the data for fine and coarse data (right panel) is also inadequate, as seen by segregation of the residuals by dataset; hence the different best-fit parameters for each grain size fraction are considered as genuine.

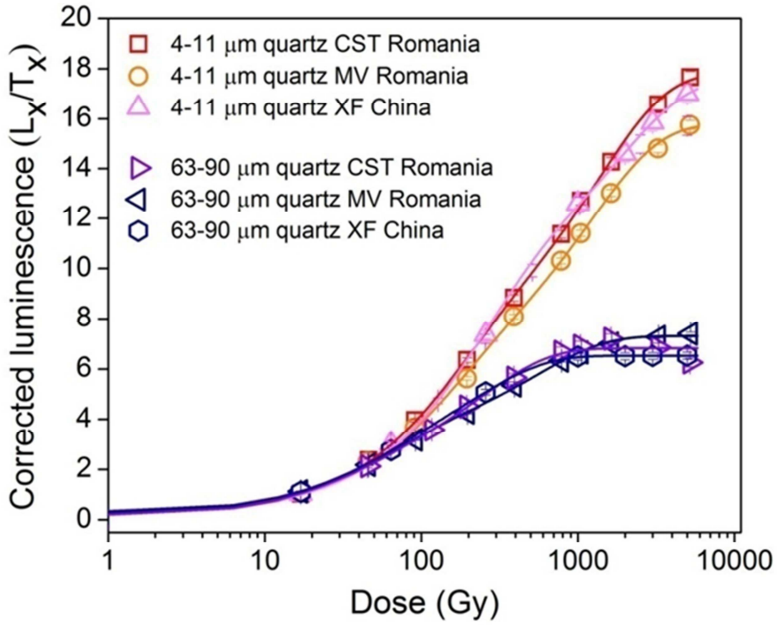

FIGURE 3. Representative SAR dose response curves for fine (4-11 μm) and coarse (63-90 μm) quartz from Romanian loess and Chinese loess.

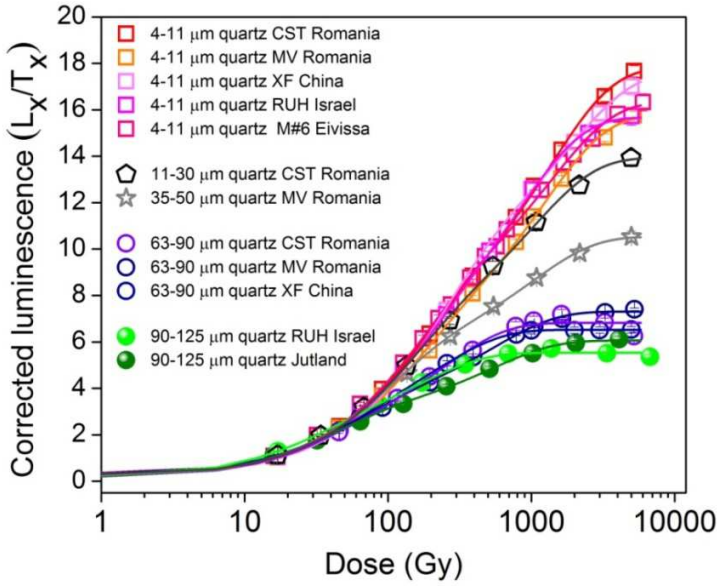

FIGURE 4. Representative SAR dose response curves of quartz of different grain sizes and origins.

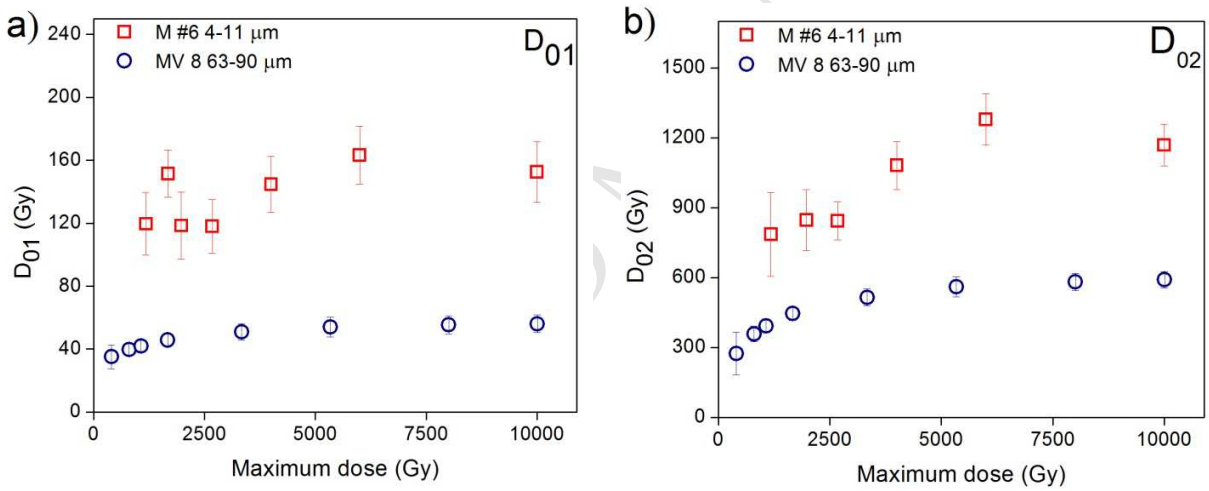

FIGURE 5 – Comparison of D_0 values for D_{01} (a) and D_{02} (b) obtained for fine (M#6) and coarse grains (MV8) of quartz as function of the maximum given dose.

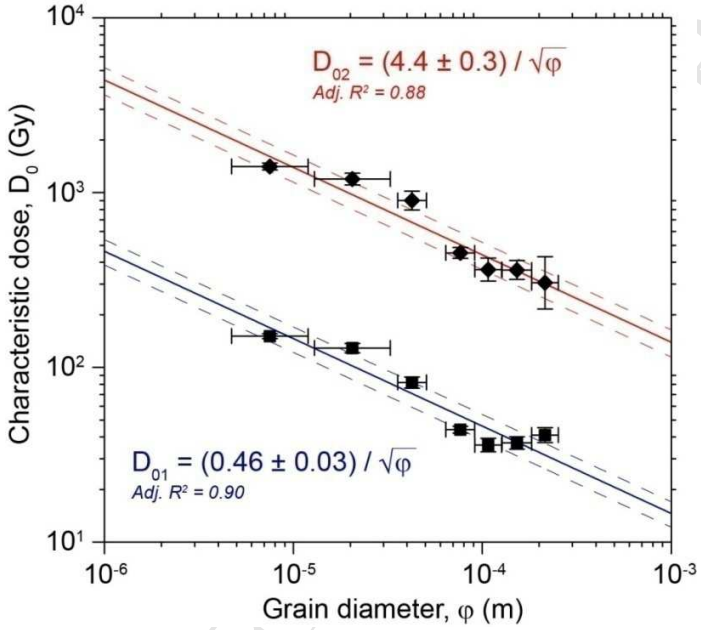

FIGURE 6. Variation of saturation characteristics (D_0 parameters) as function of grains size. Please note the log-log scale.